Intelligent Energy Management based on an Optimistic Strategy for a Hybrid PV/Tidal System without Storage

HAZEM ZRIBI, AICHA ABID, MOUNA BEN HAMED
Electrical Department of Engineering L/R:
Processes, Energy, Environment, and Electrical
Systems (PEESE),
University of Gabes, National Engineering School,
Omar Khattab Street Gabes 6029,
TUNISIA

Abstract: - This work presents an intelligent energy management approach for a connected hybrid system composed of photovoltaic (PV) and tidal energy, optimized to supply electricity for the TIMAB Gabes industry. The suggested configuration enables various sources to supply power to the load either independently or concurrently, contingent upon meteorological conditions. The strategy is based on an optimistic management algorithm considering production, prioritized load consumption, and variable electricity tariffs. To do this, we first present the modeling of the different sources equipped with the controllers, allowing their production to be maximized. In the second part, the energy management algorithm is developed to guarantee a consistent allocation of energy transfers between sources, load, and the grid. The manager is finally implemented in the MATLAB/Simulink simulator. The assessment of the complete hybrid system's functionality has been conducted. The obtained results demonstrate the effectiveness of the system in ensuring reliable operation and improving the utilization of renewable energy resources, making it a suitable solution for industrial applications.

Key-Words: - Renewable Energies, Hybrid System, Photovoltaic, Tidal Turbine, Intelligent Management, Optimistic Strategy,

Received: May 11, 2025. Revised: December 23, 2025. Accepted: March 14, 2025. Published: June 11, 2026.

1 Introduction

The growing demand for sustainable and efficient energy solutions has encouraged the development of hybrid renewable energy systems. In Tunisia, the industrial sector represents a significant portion of national electricity consumption.

To meet some of their electrical needs in the absence of a grid, most factories are equipped with small thermal or gas power plants. In recent years, due to the high cost of electric power generation, many factories have begun to widely consider the use of hybrid renewable energy sources connected to the power grid, [1], [2], [3], [4], [5], [6] .

Combining different renewable energy sources improves the continuity of power supply while increasing system autonomy. Various studies have investigated hybrid configurations integrating solar, wind, hydro, and conventional energy sources. Efficient energy management strategies are essential to ensure optimal utilization of available resources and proper coordination of system operations.

In this framework, the proposed management strategy operates as an intelligent approach capable of prioritizing loads, considering tariff variations, and adapting its operation according to environmental and system conditions.

Although rule-based, its adaptive and context-aware behavior enables real-time smart operation under dynamic conditions.

The aim of this study is to examine energy management in multi-source hybrid system capabilities. To illustrate the adopted approach, the system under investigation includes a photovoltaic generator and a hydro turbine. The entire setup is tested through simulations in the Matlab/Simulink environment, [7], [8].

2 System Overview

The system integrates photovoltaic and tidal energy sources operating in a grid-connected configuration.

PV generation consists of an installed capacity of 800 kWc, organized into four independent units of 200 kW each.

- The power output accounts for temperature and irradiance (daily and seasonal effects), [9].

The tidal subsystem has a nominal capacity of 200 kW and is based on a Permanent Magnet Synchronous Generator (PMSG). Its power output is proportional to the cube of the tidal current speed, which varies with temporal and site-specific conditions.

- **Load Profile**: Consumption is categorized into three prioritized levels:
  - P1 = 840 kW: Production Units.
  - P2 = 150 kW: Shipping Units.
  - P3 = 10 kw: Outdoor Lighting and administration.
- **Electric Grid**: The system is connected to the grid for energy injection or consumption, with tariffs that vary by time-of-use [8] .

The overall architecture of the hybrid PV/tidal system is illustrated in Figure 1.

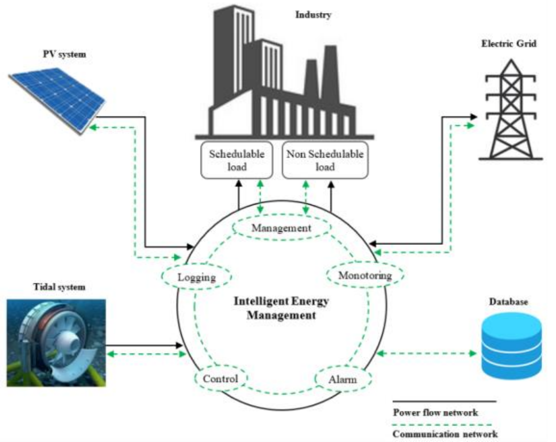

Fig. 1: System architecture with intelligent energy management
Source: created by the authors

3 Production System Model

The power delivered by the different energy sources depends on several parameters.

- For the PV generator, the temperature T and the irradiation I_r affect the supplied power.
- For the tidal turbine, the power supplied depends on the tidal speed Vtidal.

3.1 PV system Model

In this study, we selected a photovoltaic PV generator consisting of 1440 Trina Vertex_DE19_555wp PV modules arranged in 72 parallel branches and 20 modules in series. The modules are of the polycrystalline silicon type, featuring an efficiency of ηpv=18%.

Under standard operating conditions (1000 W/m^2 and 25°C), PV generator provides a power of 800 kWp. Photovoltaic production varies depending on irradiation and temperature. These two variables vary depending on the season and solar Position (q). This effect simulates the evolution of solar irradiance incident on a horizontal or inclined surface over the course of a typical day of each month, taking into account:

The day length varies throughout the year depending on the month.

- irradiance amplitude exhibits seasonal variations, with higher levels during summer.The position of the sun in the sky (hourly solar angle).

The day length Lday(m), expressed in hours, is approximated using a sinusoidal function of the month m ∈ [1,12]:

$$L_{day}(m) = 10 + 4.\sin(\tfrac{2\pi(m-6)}{12}) \quad (1)$$

The duration of daylight ranges from approximately 10 hours in winter (December–January) to 14 hours in summer (June–July).This formulation aligns longer days with the summer period. The sunrise and sunset times are derived from the calculated day length:

$$h_{sunrise} = 12 - \frac{L_{day}(m)}{2}, h_{sunset} = 12 + \frac{L_{day}(m)}{2} \quad (2)$$

A solar noon is assumed at 12 PM.The apparent solar angle q(t) is modeled as a sinusoidal function defined between sunrise and sunset.Let us consider:

$$\theta_{sun}(t) = \pi.\frac{t - h_{sunrise}}{h_{sunset} - h_{sunrise}} \; if \; h_{sunrise} \leq t \leq h_{sunset} \quad (3)$$

This ensures a gradual variation in the height of the sun in the sky.

The maximum irradiance amplitude (in kW/m²) varies monthly, reaching higher values during the summer period:

$$A_{season}(m) = 1 + 0{,}3.\cos\left(\frac{2\pi(m-6)}{12}\right) \quad (4)$$

Typical values range from approximately 1.3 kW/m² in June–July to about 0.7 kW/m² in

December–January.The global irradiance incident on the PV surface is therefore expressed as:

$$\begin{cases} G(t,m) = A_{season}(m).\sin\theta \quad if \quad t\epsilon[h_{sunset}, h_{sunrise}] \\ G(t,m) = 0 \quad at\ night \end{cases} \quad (5)$$

To account for all these influences, we used the Fuentes mathematical model to evaluate the output power of the photovoltaic generator, represented by the following equation, [9], [10], [11]:

$$P_{PV}(t) = P_{PV-ref}.G(t,m).\left[1-\gamma(T(t)-T_{ref})\right] \quad (6)$$

where:

- P_{PV-ref} represents the reference of output power at (1000 W/m^2 and 25°C).
- γ is the temperature influence coefficient on PV power, assumed to be constant, with a value for silicon cells that falls within the range of (0.0035 to 0.0050) °C^{-1}.

T represents the cell junction temperature (in °C), with a reference value of 25°C.

Under standard test conditions (STC), the PV system operates at Vmpp = 636 V and Impp = 1256.4 A.

The peak power is approximately P_{mpp}=800 kWc.

The current–voltage and power–voltage characteristics of the PV generator under varying temperature and irradiance are shown in Figure 2.

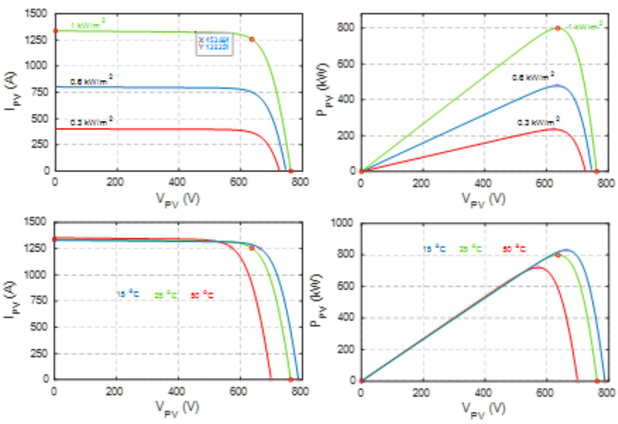

Fig. 2: I-V and P-V characteristics of the PV generator with irradiation and temperature variation
Source: created by the authors

3.2 Tidal System Model

In this study, we examined a tidal system linked to a permanent magnet synchronous generator. The power potential of tidal currents can be derived using the same formula applicable to wind energy systems, [12], [13], [14].

$$P_{tid} = 0{,}5.\rho.\pi.R^2.C_p(\lambda,\beta).{V_t}^3(t) \quad (7)$$

where:

ρ is the sea water density approximately equal to 1025 kg/ m^3, R is the radius of the blades of the hydro turbine (m^2), V_t is the tidal current speed (varies with time and region) and C_p is the power coefficient.

The power coefficient C_P (β, λ) (Figure 3), is a nonlinear function of the tip speed ratio l and the pitch angle b given by:

$$C_p(\lambda,\beta) = 0{,}5176\left(\frac{116}{\lambda_i} - 0{,}4.\beta - 5\right)e^{-\left(\frac{21}{\lambda_i}\right)} + 0{,}0068.\lambda \quad (8)$$

where:

$$\frac{1}{\lambda_i} = \frac{1}{\lambda + 0{,}008\beta} - \frac{0{,}035}{\beta^3+1} \quad (9)$$

The nonlinear variation of the power coefficient Cp with the tip speed ratio and pitch angle is shown in Figure 3.

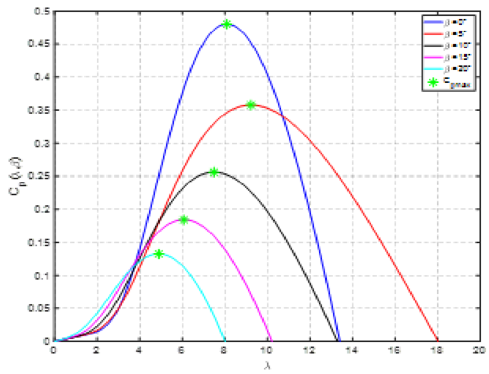

Fig. 3: Typical C_P versus (λ,β) curve
Source: created by the authors

The Tip Speed Ratio (TSR) is defined as:

$$\lambda = \frac{R\Omega_t}{V_t} \quad (10)$$

From the relations (7), (8) and (10), the mechanical power of the turbine can be expressed by:

$$P_{hyd} = \frac{1}{2.\lambda^3}.\rho.\pi.C_p.R^5.{\Omega_t}^3 \quad (11)$$

The relationship between the turbine power and tidal speed at maximum output power (Figure 4) is given by:

$$P_{hyd-max} = \left[\frac{1}{2.\lambda^3{}_{opt}}.\rho.\pi.C_{popt}.R^5\right]\Omega_t{}^3 = k_{opt}\Omega_t{}^3 \quad (12)$$

Figure 4 shows the relationship between the mechanical power of the tidal turbine and its rotational speed.

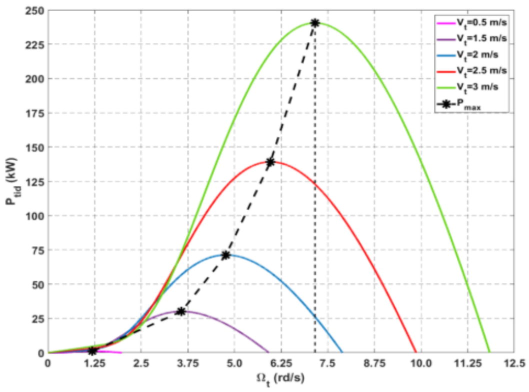

Fig. 4: Turbine power vs mechanical angular velocity characteristic

Source: created by the authors

4 Optimistic Energy Management Algorithm

4.1 Methodology

The conditional rules of the deterministic energy manager take into account:

The excess of generated energy, defined as the difference between production and consumption,

The operating period (off-peak, normal, and peak)

- ✓ The purchase and sale price of kWh,
- ✓ The profitability threshold for injecting or consuming from the grid.

For a production plant, such as the TIMAB Gabès company (chemical industry, high energy consumption), the definition of time periods (off-peak, normal, peak) must consider:

1. The industrial pricing profile of STEG (electricity supplier in Tunisia)
2. The periods of high activity within the factory (shift work, maintenance, etc.)
3. The cost of energy during peak periods, which is often higher.

The definition of industrial time periods is generally based on the tariff ranges of STEG. The following table provides the different periods and the corresponding time ranges:

Table 1. Definition of Industrial Time Periods

Period	Hours	Description
Off-Peak	22h00 – 06h00	Low rates, often utilized for starting heavy machinery
Normal	06h00 – 17h00	Continuous activity, standard production
Peak	17h00 – 22h00	Critical period, high rates, often to be avoided

Source: created by the authors

4.2 Load Priority Strategy

The algorithm allocates available energy according to load priority:

- ✓ If: $P_{prod}(t) \geq (P_1 + P_2 + P_3)$ All loads are satisfied, then inject the surplus into grid
- ✓ else:
  - Priority 1 (P_1) is always supplied first.
  - Then Priority 2 (P_2), if sufficient energy remains.
  - Lastly, Priority 3 (P_3), only if surplus is available.

Where:

$$P_{load}(t) = P_1(t) + P_2(t) + P_3(t) \quad (13)$$

4.3 Energy Manager Conditional Rules

The conditional rules for a deterministic manager in an industrial production facility such as TIMAB Gabes must consider:

- ✓ The STEG tariff ranges (off-peak / normal / peak).
- ✓ Production priorities (continuous, flexible).
- ✓ Possible solar self-consumption,
- ✓ Critical vs. non-critical loads.

The input variables for the deterministic manager are:

1.Hybrid production (PV / Tidal):

$$P_{prod}(t) = P_{pv}(t) + P_{tid}(t) \quad (14)$$

2.Factory consumption:

$$P_{load}(t) = P_1(t) + P_2(t) + P_3(t) \quad (15)$$

3.Time period: Off-peak / Normal / Peak.

The output actions (energy strategy) are:

1. Inject (surplus to the grid)
2. Self-consume (prioritize internal use)
3. Reduce non-critical loads (if energy is expensive and voltage is critical)

The following table illustrates the conditional rules of the manager.

The optimistic strategy presumes the most favorable availability of renewable resources and the flexibility of the grid. The algorithm functions in the following manner:

✓ Calculate total available powers:

$$P_{prod}(t) = P_{pv}(t) + P_{tid}(t) \quad (16)$$

The available power is compared with the demand thresholds (P1, P2, P3).

The electricity tariff period is then identified as follows:

- '*Night*': low cost
- '*Day*': normal rate
- '*Summer Peak*': highest rate
- '*Winter Peak*': intermediate rate

✓ Decision logic:

- If $P_{prod}(t) > P_{cons}(t)$, consume locally and inject surplus if the grid allows.
- If $P_{prod}(t) < P_{cons}(t)$, supplement from the grid considering cost-efficiency:
  - Prefer local production during peak periods.
  - Purchase during low-cost periods (e.g., night).
  - Decision taking into account tariffs

The tariff periods used in the decision logic (‘Night’, ‘Day’, ‘Summer Peak’, and ‘Winter Peak’) correspond to the industrial STEG time-of-use classification presented in Table 1. Specifically, the ‘Night’ period coincides with the Off-Peak range (22:00–06:00), the ‘Day’ period corresponds to the Normal range (06:00–17:00), while the ‘Summer Peak’ and ‘Winter Peak’ periods represent seasonal distinctions of the Peak range (17:00–22:00) according to electricity pricing policies.

The extraction of energy from the grid may be restricted according to the prices of kWh purchases.

The tariff-aware decision rules associated with the proposed energy management strategy are summarized in Table 2.

Table 2. Tariff-Aware Decision Table

Period	Injection condition	Grid usage condition
Night	If surplus > 200 kW	Allowed (low price)
Day	Inject if surplus > 200 kW	Limited if $P_{prod}(t) < P_1(t)$
Summer Peak	Inject all surplus	Minimize usage (very high rate)
Winter Peak	Inject only if excess high	Moderate grid use

Source: created by the authors

The detailed flowchart of the proposed deterministic energy management algorithm is presented in Figure 5.

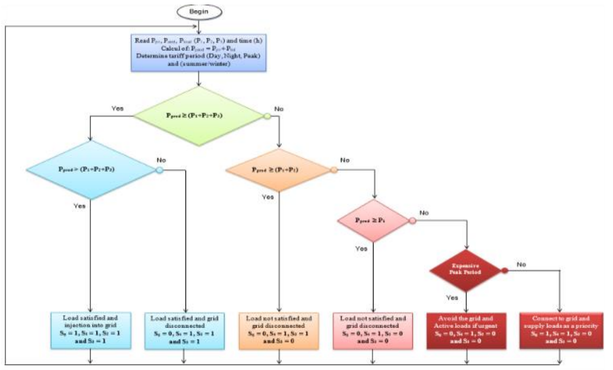

Fig. 5: Flowchart of the deterministic management algorithm
Source: created by the authors

5 Deterministic Operation Scenarios

5.1 Scenario 1: Full Renewable Supply (High Solar + High Tidal) and High consumption

- Time: Summer midday (high irradiance and tidal peak)
- $P_{pv} = 800kW, P_{tid} = 200kW \longrightarrow P_{prod} = 1000kW$
- Load requirement: $P_1 + P_2 + P_3 = 1000$ kW
- Grid is used minimally to supply the remaining 50 kW, as tariffs are moderate during the day.

The daily meteorological variations used in Scenario 1 are shown in Figure 6.

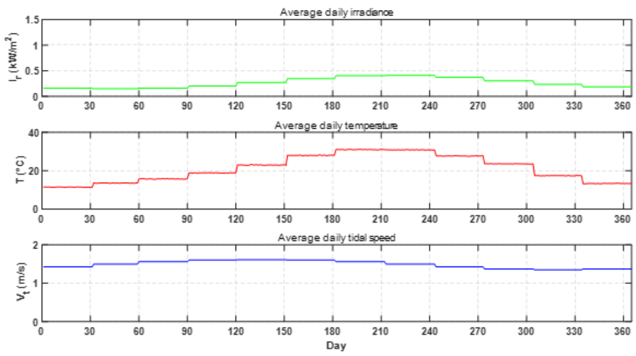

Fig. 6: Evolution of daily average metrological quantities (1st scenario)
Source: created by the authors.

The monthly evolution of production and load for Scenario 1 is presented in Figure 7.

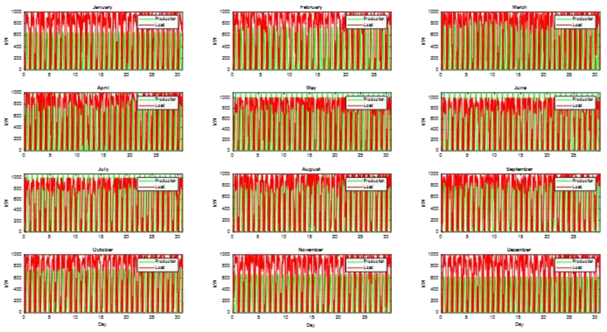

Fig. 7: Evolution of monthly production and load (1st scenario)
Source: created by the authors

The dynamic behavior of the hybrid system over a typical day is presented in Figure 8.

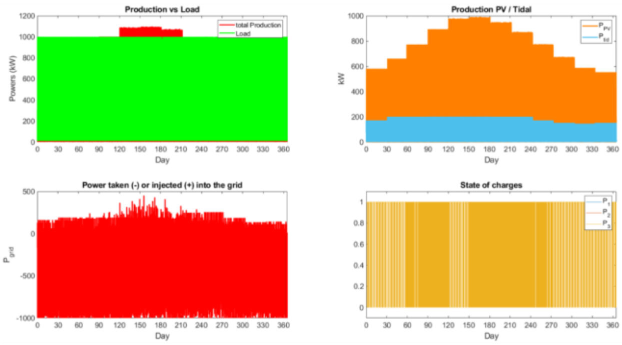

Fig. 8: Evolution of daily production vs load, production PV/Tidal, Power of grid, and state of load (1st scenario)
Source: created by the authors

The monthly and annual energy exchanges with the grid are presented in Figure 9a and Figure 9b, respectively.

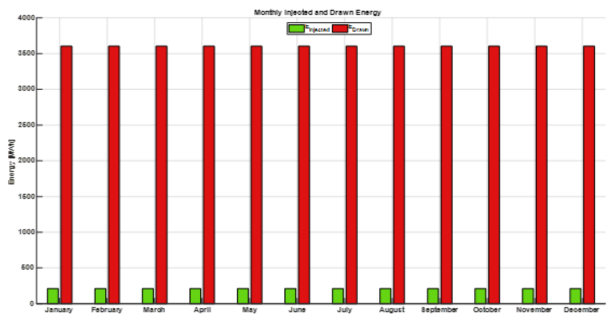

Fig. 9a: Monthly injected and drawn Energy (1st scenario)
Source: created by the authors

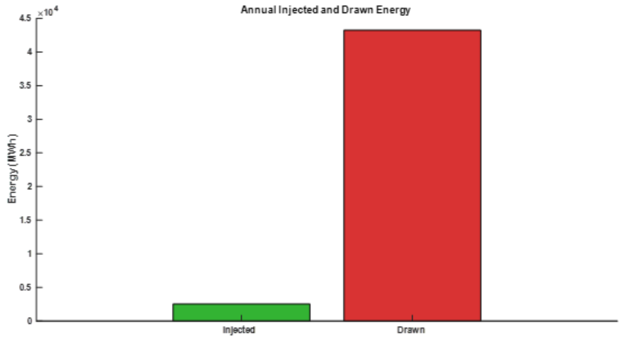

Fig. 9b: Annual injected and drawn Energy (1st scenario)
Source: created by the authors

The results shown in Figure 6 and Figure 9 indicate that power generation follows the expected solar profile, with a peak around midday. Maximum production is observed during the summer period (May–August), while lower values occur in winter (December–February) due to reduced irradiance levels. The load remains relatively stable, typically ranging between 600 and 900 kW, which reflects the characteristics of an industrial consumption profile.

A slight increase in load demand is observed during the summer period, which may be associated with higher industrial activity or cooling requirements. In terms of the production–demand balance, several months (January, February, November, and December) show that production remains below demand, leading to increased dependence on the grid.

Regarding the variability of production, it is observed that cloudy days or low tide periods can be indicated by dips in the red curve. This reflects a more pronounced daily fluctuation compared to the load, highlighting the importance of enhancing the intelligent manager.

In conclusion, it can be asserted that the system operates in an optimized manner. It first addresses the priority loads (P1), and subsequently activates the secondary loads if production or pricing allows. It is also observed that summer is conducive to autonomy (production > load), resulting in a net injection into the grid.

Conversely, during winter, the installation remains heavily reliant on the grid, particularly in instances of low solar production.

Scenario 2: High renewable production (maximum PV and high tidal) with reduced load demand

- $P_{pv} = 800kW, P_{tid} = 200kW \longrightarrow P_{prod} = 1000kW$

The total demand of the three loads (P1, P2, and P3) is reduced to 500 kW.

Figure 10 illustrates the monthly variation of production and load for Scenario 2.

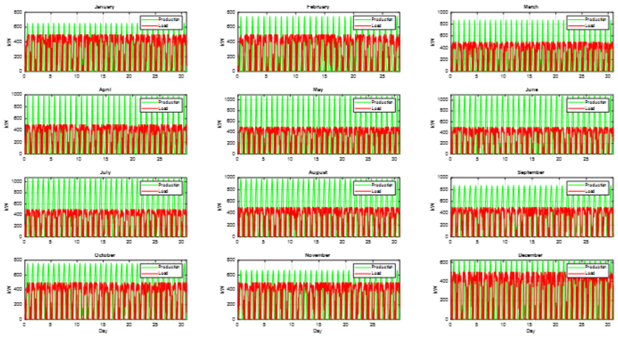

Fig. 10: Evolution of monthly production and load (2nd scenario)
Source: created by the authors

The daily profiles of power generation and consumption for Scenario 2 are presented in Figure 11.

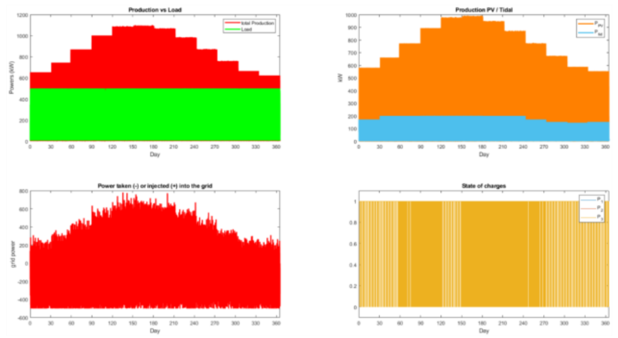

Fig. 11: Evolution of daily production vs load, production PV/Tidal, Power of grid and state of load (2nd scenario)
Source: created by the authors

The corresponding monthly and annual energy exchanges with the grid are presented in Figure 12a and Figure 12b.

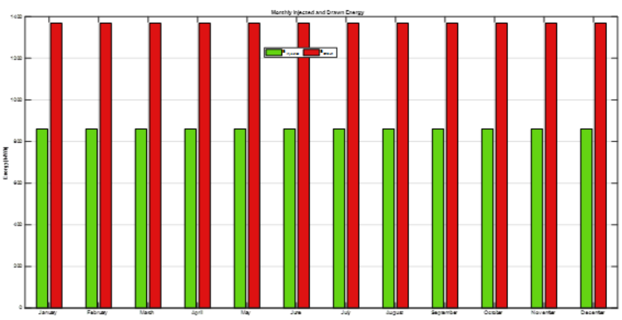

Fig. 12a: Monthly Injected and Drawn Energy (2nd scenario)
Source: created by the authors

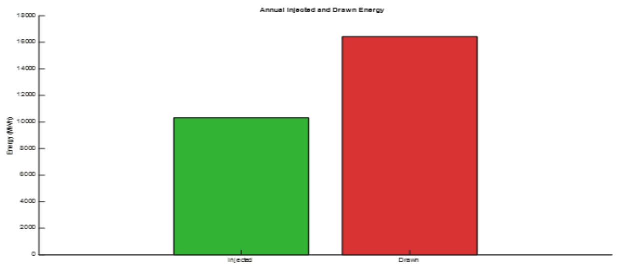

Fig. 12b: Annual injected and drawn energy (2nd scenario)
Source: created by the authors

In this scenario, the system generates more energy than is required. The reduced demand means that half of the production is fed into the gridIn this configuration, the energy demand is fully supplied by renewable sources without requiring grid support for local consumption.

These results confirm the feasibility of a fully renewable supply, while highlighting the need for better matching between production and consumption levels.

5.2 Scenario 3: Deficit Period (High Solar + Tidal turbine broken down)

- Time: Early morning winter (low irradiance and high tide)
- $P_{pv} = 800kW, P_{tid} = 0kW \longrightarrow P_{prod} = 800kW$
- Load requirement: $P_1 + P_2 + P_3 = 1000$ kW

The daily meteorological parameters for Scenario 3 are shown in Figure 13.

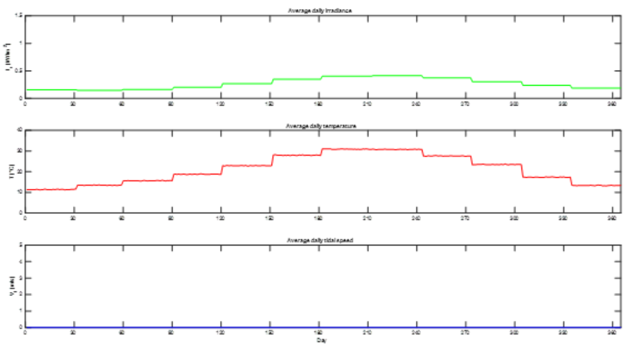

Fig. 13: Evolution of daily average metrological quantities (3st scenario)
Source: created by the authors

The monthly behavior of production and load for Scenario 3 is illustrated in Figure 14

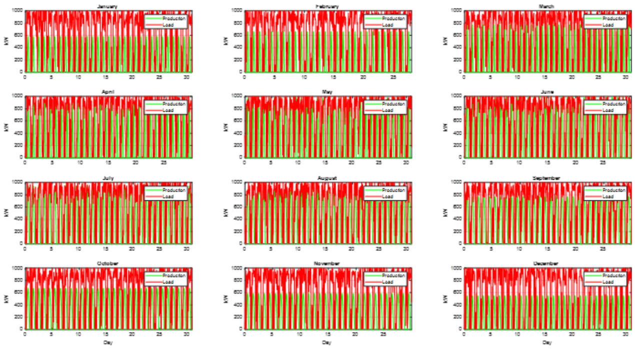

Fig. 14: Evolution of monthly production and load (3^{rd} scenario)
Source: created by the authors

The daily comparison of renewable generation, load, and grid power in Scenario 3 is presented in Figure 15.

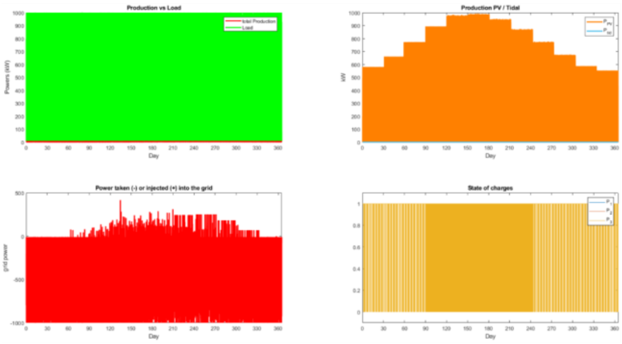

Fig. 15. Evolution of daily production vs load, production PV/Tidal, Power of grid, and state of load (3^{rd} scenario)
Source: created by the authors

The monthly and annual injected and drawn energies for Scenario 3 are shown in Figure 16a and Figure 16b.

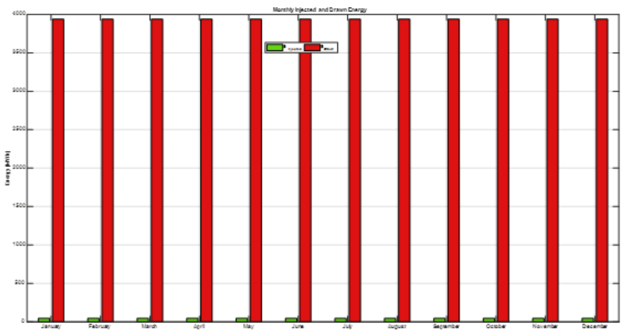

Fig. 16a: Monthly injected and drawn energy (3^{rd} scenario)
Source: created by the authors

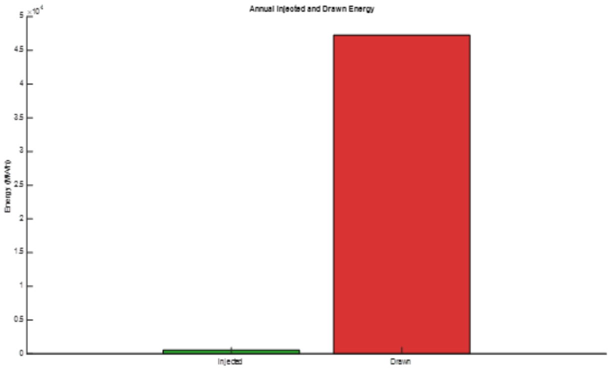

Fig. 16b: Annual injected and drawn energy (3^{rd} scenario)
Source: created by the authors

In this scenario, the system operates under an energy deficit despite the high installed solar capacity.

The outage of the hydrokinetic turbine highlights a system vulnerability and results in increased dependence on the grid.

The energy management strategy prioritizes critical loads (P1) while reducing secondary loads to maintain system stability.

6 Conclusion

This article presents a smart energy management strategy tailored for hybrid renewable systems that combine photovoltaic (PV) sources and hydropower, without relying on energy storage.

The proposed strategy is based on an optimistic deterministic control logic, which allows for:

- Prioritizing internal consumption based on the significance of loads (production units, logistics, administrative services),
- Dynamically adapting to the daily and seasonal variability of renewable production (solar irradiation, tides),
- Considering hourly electricity rates, avoiding consumption during peak periods, and favoring injection or network support during off-peak hours.

The optimistic philosophy of the algorithm aims to maximize the self-consumption of available green energy. It intelligently activates loads based on renewable production while reducing dependence on the grid, particularly during high-cost periods. Even under production deficit conditions, such as low irradiance periods or turbine outages, the strategy ensures the continuity of priority loads through controlled use of grid support.

The proposed approach provides a practical and scalable solution for energy management in industrial applications based on renewable sources, particularly in the absence of storage systems. It promotes efficient use of renewable energy while ensuring reliable interaction with the grid. Although based on deterministic rules, the strategy adapts to variations in renewable generation and tariff conditions. Future developments will focus on improving system performance by integrating advanced control techniques such as fuzzy logic, reinforcement learning, or model predictive control.

References:

[1] Himadry Shekhar Das, Yatim, A.H.M, Tan,Chee Wei, Lau,Kwan Yiew , Proposition of a PV/tidal powered micro-hydro and diesel hybrid system, *Renewable and Sustainable Energy Reviews*, Vol. 53, 2016, pp. 1137–1148. DOI: 10.1016/j.rser.2015.09.038.

[2] Peter Osman, Jennifer A.Hayward, Irene Penesis, Philip Marsh, Mark A.Hemer, David Griffin, Saad Sayeef, Jean-Roch Nader, Remo Cossu, Alistair Grinham, Uwe Rosebrocck and Mike Herzfeld , Dispatchability, Energy Security, and Reduced Capital Cost in Tidal-Wind and Tidal-Solar Energy Farms, *Energies*, Vol. 14, No. 24, 2021. DOI: 10.3390/en14248504..

[3] Muhammad Fahad Zia, Mashood Nasir, Elhoussin Elbouchikhi, Mohamed Benbouzid, Juan C. Vasquez, Josep M. Guerrero, Energy management system for a hybrid PV-Wind-Tidal-Battery-based islanded DC microgrid: Modeling and experimental validation, *Renewable and Sustainable Energy Reviews*, Vol. 159, No. 112093, 2022. DOI: 10.1016/j.rser.2022.112093.

[4] Jonathan Cohen, Michael B. Kane, Alexia Marriott, Franklin Ollivierre, Krissy Govertsen, Economic controls codesign of hybrid microgrids with tidal/PV generation and lithiumion/flow battery storage, *Energies*, Vol.16, No. 2761, 2023. https://doi.org/10.3390/en16062761.

[5] Chouaib Ammari, Djamel Belatrache, Batoul Touhami, Salim Makhloufi, Sizing, optimization, control and energy management of hybrid renewable energy system, *Energy and Built Environment*, Vol.3, No.4, 2022, pp. 399-411. DOI: 10.1016/j.enbenv.2021.04.002.

[6] Angel A Recalde et Manuel S. Alvarez-Alvarado, Design optimization for reliability improvement in microgrids with wind – tidal – photovoltaic generation, *Electric Power Systems Research*, Vol.188, No. 106540, 2020. DOI: 10.1016/j.epsr.2020.106540.

[7] Olivier Gauvin-Tremblay, Guy Dumas, Hydrokinetic turbine array analysis and optimization integrating blockage effects and turbine-wake interactions, *Renewable Energy*, Vol.181, 2022, pp. 851-869. DOI: 10.1016/j.renene.2021.09.003.

[8] Vikas Khare, Miraj Ahmed Bhuiyan, Tidal energy-path towards sustainable energy: A technical review, *Cleaner Energy Systems*, Vol.3, No.100041, 2022. DOI: 10.1016/j.cles.2022.100041.

[9] Meng Lin, Clemens Suter, Stefan Diethelm, Jan Van herle, Sophia Haussener, Integrated solar-driven high-temperature electrolysis operating with concentrated irradiation, *Joule*, Vol.6, No.9, 2022, pp. 2102-2121. DOI: 10.1016/j.joule.2022.07.013.

[10] Wen-Chang Tsai, Chia-Sheng Tu, Chih-Ming Hong, Whei-Min Lin, A Review of State-of-the-Art and Short-Term Forecasting Models for Solar PV Power Generation, *Energies*, Vol.16, No.14, 2023 https://doi.org/10.3390/en16145436.

[11] Kim, Jae-Kyeong and Kang, Jiseong and Shim, Jae Woong and Kim, Heejin and Shin, Jeonghoon and Kang, Chongqing and Hur, Kyeon, Dynamic Performance Modeling and Analysis of Power Grids With High Levels of Stochastic and Power Electronic Interfaced Resources, *Proceedings of the IEEE*, Vol.111, No.7, 2023, pp. 854-872. DOI: 10.1109/JPROC.2023.3284890.

[12] M. Nachtane, M. Tarfaoui, I. Goda, M. Rouway, A review on the technologies, design considerations and numerical models of tidal current turbines, *Renewable Energy*, Vol.157, 2020, pp. 1274-1288. DOI: 10.1016/j.renene.2020.04.155.

[13] Ladislas Mutunda Kangaji, Atanda Raji, Efe Orumwense, Optimizing Sustainability Offshore Hybrid Tidal-Wind Energy Storage Systems for an Off-Grid Coastal City in South Africa, *Sustainability*, Vol.16, No.21, 2024. DOI: 10.3390/su16219139.

[14] Simon P. Neill, Kevin A. Haas, Jérôme Thiébot, Zhaoqing Yang, A review of tidal energy Resource, feedbacks, and environmental interactions. *J. Renewable Sustainable Energy*, Vol.13, No.6, 2021. DOI: 10.1063/5.0069452.

Contribution of Individual Authors to the Creation of a Scientific Article (Ghostwriting Policy)

- Hazem Zribi developed the energy management system, carried out the simulations, analyzed the results, and wrote the manuscript.
- Aicha Abid contributed to proofreading and verification of the manuscript.
- Mouna Ben Hamed supervised the work, verified the results, and provided final approval.

Sources of Funding for Research Presented in a Scientific Article or Scientific Article Itself

No funding was received for conducting this study.

Conflict of Interest

The authors declare that they have no conflicts of interest relevant to the content of this article.